ISSN 0016-7932, Geomagnetism and Aeronomy, 2015, Vol. 55, No. 2, pp. 210–218. © Pleiades Publishing, Ltd., 2015.
Original Russian Text © I.A. Kornilov, T.A. Kornilova, I.V. Golovchanskaya, 2015, published in Geomagnetizm i Aeronomiya, 2015, Vol. 55, No. 2, pp. 222–230.

On the Physical Nature of Auroral Breakup Precursors as Observed in an Event on 5 March 2008[1]

I. A. Kornilov, T. A. Kornilova, and I. V. Golovchanskaya
Polar Geophysical Institute, 26a, Academgorodok, Apatity, 184200 Russia
e-mail: kornilov@pgia.ru, golovchanskaya@pgia.ru

Received May 29, 2014; in final form July 16, 2014

Abstract—Using coordinated THEMIS spacecraft and all-sky imager observations, we studied an auroral breakup event on 5 March 2008, where auroral activities for 30–40 min before T_0 were all of the East-West (E-W) orientation, and found that their dynamics infers a wave process. For the event under study, there were conjunctive measurements (with 3 s time resolution) of plasma, energetic particles, magnetic B and electric E fields by four THEMIS probes, positioned approximately along the tail. The THEMIS probe measurements, bandpass-filtered in the range 12–120 s, revealed the low-frequency wave activity in the considered time interval. The out-of-phase relation between variations in the magnetic and plasma pressures, along with a positive correlation between $-\partial Bx/\partial t$ and z GSM component of ion velocity (flapping), indicated the ballooning mode. Considering the similarity of the wave-like characteristics derived from ground-based auroral and THEMIS spacecraft observations, we argue that the E-W auroral features preceding onset may be related to ballooning waves propagating in the plasma sheet, their wavefronts inclined at relatively small angles to the azimuthal direction. The implications for mechanisms of substorm triggering are discussed.

DOI: 10.1134/S0016793215020103

1. INTRODUCTION

Since the study of Akasofu (1964), the physics of magnetospheric substorm, i.e., a large-scale magnetospheric reconfiguration accompanied by a huge release of stored magnetic energy, has been much elucidated, however the mechanism of a transition to the substorm expansion phase is not yet fully understood. In this connection, optical observations of auroral onset and especially of its precursors are of great importance, for they may be indicative of the processes triggering expansion of magnetic dipolarization in the magnetosphere (Akasofu et al., 2010).

In the last few decades, much attention was paid to auroral breakup precursors visualized in all-sky images as roughly North-South aligned (N-S) auroral features originating at the poleward auroral boundary, presumably in association with the Poleward Boundary Intensifications (PBIs), and progressing equatorward (Rostoker et al., 1987; Henderson et al., 1998; Nishimura et al., 2010). These N-S forms are usually considered as ionospheric signatures of the fast plasma flows in the magnetotail (e.g., Baumjohann et al., 1989), whose azimuthal extent is narrow (1–3R_E).

At the same time, a different type precursor activities is well-known, when slightly inclined to the geomagnetic latitudinal direction (hereafter E-W) auroral forms appear at high latitudes (sometimes in connection with PBIs), and start propagating to lower latitudes, where under certain conditions they are getting involved in the auroral breakup development (Oguti, 1973; Kornilova et al., 2006, 2008; Mende et al., 2011; Kornilova et al., 2012). In this case, one of preexisting E-W arcs or (as in the event here considered) of propagating from poleward E-W arcs becomes the prebreakup arc, along which breakup initiates. The events, which show only E-W auroral features prior to breakup onset, were distinguished by Mende et al. (2011) in a special class of so-called E-W events. It was also noted by Mende et al. (2011) that E-W arcs are standard, well-documented features of presubstorm auroras.

The E-W type auroral activities preceding onset is a subject of this study. In what follows we present the THEMIS all-sky auroral imagery for an E-W event on 05 March 2008 (Section 2), search for the magnetospheric counterpart to the E-W auroral precursors of onset in the conjunctive measurements of the THEMIS probes and argue that these precursors may be related to the ballooning waves propagating in the plasma sheet at that time (Section 3). The implications for mechanisms of substorm triggering are discussed in Section 4.

2. EAST-WEST TYPE PRECURSOR ACTIVITIES PRIOR TO ONSET AS INFERRED FROM GROUND-BASED OPTICAL OBSERVATIONS

Here we illustrate the main features of auroral breakup precursors in an event on 05 March 2008 (the

[1] The article was translated by the authors.

onset identified by optical observations was at T_0 = 0604:00 UT). It was verified by mosaic constructed from THEMIS all-sky auroral images [http://themis.ssl.berkeley.edu/gbo/] that during 40 minutes prior to breakup, the observed auroral features were all of the E-W orientation, none of the images revealing N-S structures. Thus the event under study is an E-W event, according to the Mende et al. (2011) classification.

The mosaic constructed for T_0 and projected on the geographic map is shown in Fig. 1a. The images of the stations composing the mosaic were filtered and arranged as avi-films to highlight weak auroral activities preceding onset. An avi-film made by observations of a Canadian station GILL in the time range 0550–0615 UT is available at ftp://pgia.ru/kornilov/gill.avi. The time of the movie is 60 times compressed compared to the real time. A distinctive feature of the auroral activities, being investigated, is their wave-like character. The propagation of the auroral structures is nearly equatorward (actually the wavefronts are slightly inclined to the E-W direction). Occasionally, inhomogeneities inside the auroras intensify and develop rapid azimuthal motions previously described by Uritsky et al. (2009) as longitudinally propagating arc waves. The direction of azimuthal propagation is predominantly westward (Uritsky et al., 2009).

Wave-like processes in the auroral dynamics before onset is a frequently observed phenomenon, which manifests in other events (see avi-films at ftp://pgia.ru/kornilov/22030114.avi made by TV all-sky observations at Lovozero station).

The original and filtered N-S keograms constructed by auroral observations of GILL station (56.4° N, 265.3° E geographic coordinates, 0634 UT magnetic midnight), which is central in the mosaic (Fig. 1a), are displayed in Fig. 1b and Fig. 1c, respectively.

In the filtered keogram (Fig. 1c), one can see the poleward auroral boundary and its occasional intensifications, as well as slanted auroral traces indicating equatorward propagating auroras (their E-W elongation can be verified by the movie). It is also seen that some of the auroral traces initiate from the PBIs).

In Fig. 1d, representative filtered TV all-sky images for the time interval from $T_0 - 7$ min to $T_0 + 3$ min are shown, which illustrate prebreakup auroral activities more in detail.

3. COMPARISON OF OPTICAL OBSERVATIONS WITH CONJUNCTIVE THEMIS SPACECRAFT MEASUREMENTS

For the studied event, there was a magnetic conjunction of the ground-based optical observations with in-situ THEMIS probe measurements (with 3 s time resolution) of plasma and particles, as well as of electric and magnetic fields. Around T_0 = 0604:00 UT, four THEMIS probes (*P*1, *P*2, *P*3, *P*4) were located as follows: *P*1 (–19.33, +4.91, –1.65) R_E, *P*2 (–15.72, +4.85, –2.33) R_E, *P*3 (–10.94, +3.95, –1.88) R_E, *P*4 (–10.53, +4.79, –1.85)$R_{E.}$, GSM coordinates. Their footprint locations obtained by T96 are drawn on the mosaic in Fig. 1a.

We examined the probe measurements in the time interval of interest (0520–0620 UT) and found that the probes detected low-frequency plasma oscillations with 1–2 min periods with embedded larger-amplitude wave packets. This is clearly seen in Fig. 2 in the time series of magnetic and plasma pressures (shown by the grey and black lines, respectively) bandpass-filtered in the range 12–120 s. The variations δP_{magn} and δP_{plasma} appear out-of-phase. Furthermore, as seen in Fig. 3c and 3g, the time derivative $-\partial Bx/\partial t$ (grey lines) varies in phase with the *z*-component of plasma velocity (black lines), indicating vertical motions (flapping) of the plasma sheet. These are well-known features of ballooning type perturbations (Miura et al., 1989; Ohtani and Tamao, 1993; Liu, 1997; Mazur et al., 2013).

We have tested the observed ballooning perturbations for signatures of the kinetic ballooning/interchange instability proposed by Pritchett and Coroniti (2010, 2011) and reported for a bent plasma sheet by Panov et al. (2012). This instability leads to the formation of radially elongated structures with a large length-to-width ratio (so-called, ‘fingers’). However, in contrast to what is expected for the kinetic ballooning/interchange instability (Pritchett and Coroniti, 2010, 2011), there is no steady growth in time of the amplitude of fluctuations (Fig. 2 and Fig. 3), the magnetic oscillations do not reveal a pronounced sawtooth structure (Fig. 3a and Fig. 3e), there is no correlation between Bx oscillations and variations in the electron velocity (Fig. 3a, 3d and Fig. 3e, 3h), etc. More importantly, in the conjugate auroral observations, there are no N-S structures, which could be identified as auroral manifestations of the instability ‘fingers’. Thus we conclude that in the E-W events the kinetic ballooning/interchange instability cannot have a substantial role.

As follows from Fig. 4c and 4g, in the considered time interval there were no signatures of dipolarizations/injections either. Therefore, the perturbations cannot be related to these processes.

It is seen in Fig. 4a and 4e that the observed fluctuations pronouncedly modulate the integral energy flux of 100 eV–30 keV electrons, the modulation depth being 30–40%, which should manifest in the auroral structuring.

We also verified what would be the *x*-component of the velocity of ballooning perturbations *x* if they were merely transported by the ambient plasma flow. Figures 4d and 4h show that this velocity would be less than ~ 20 km/s, which appears 1.5–2 times lower than that determined from the time lags between the probes (~ 46.5 km/s between *P*2 and *P*3, and ~ 30.5 km/s

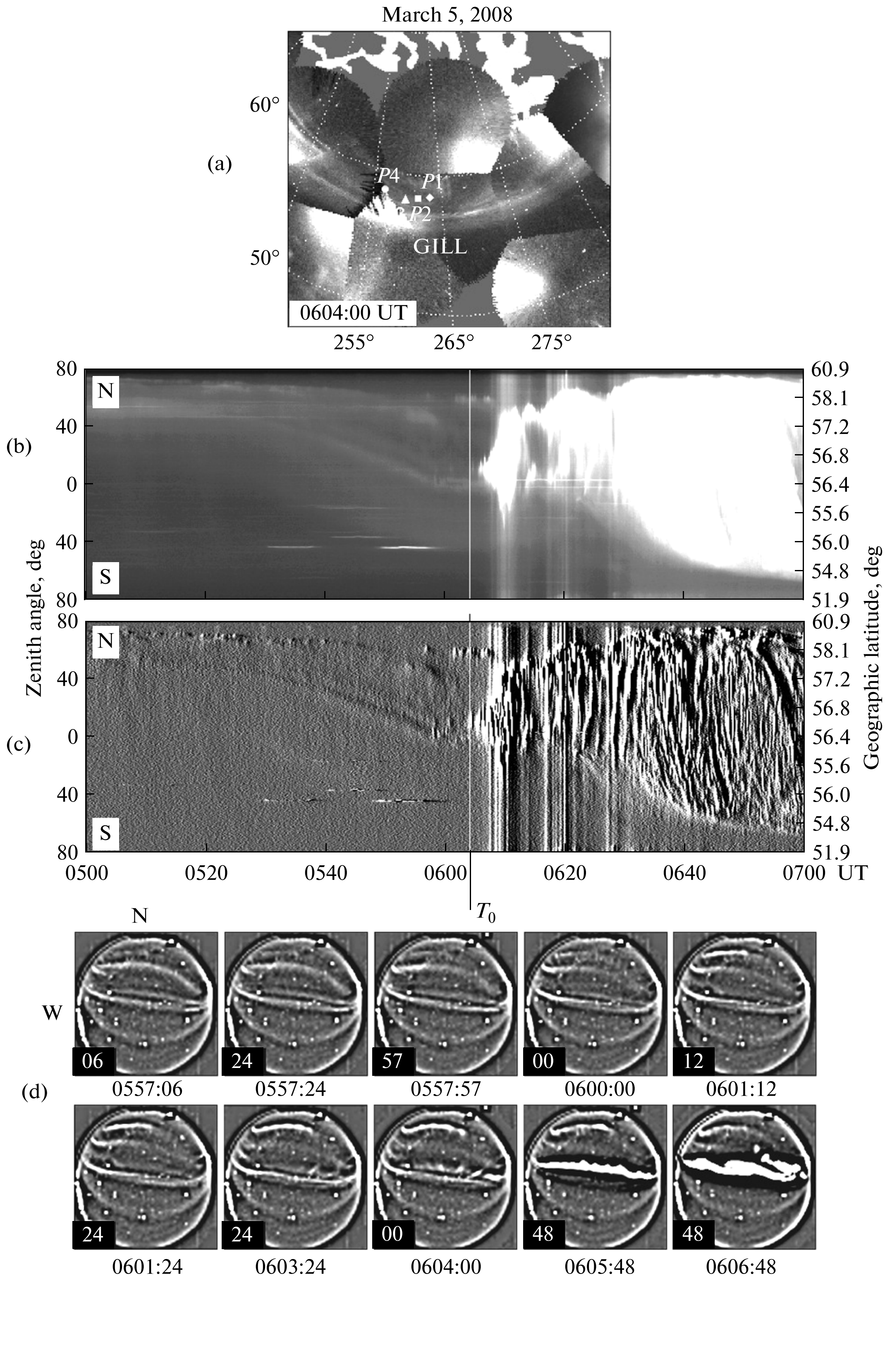

Fig. 1. Auroral data for the event of 5 March, 2008: (a) a fragment of mosaic constructed by the ground-based optical data from THEMIS Mission; the footprint locations of $P1$–$P4$ probes are marked by different symbols (circle, triangle, square, and diamond, respectively); (b) and (c) original and filtered keograms from GILL station; (d) filtered all-sky images obtained at GILL station.

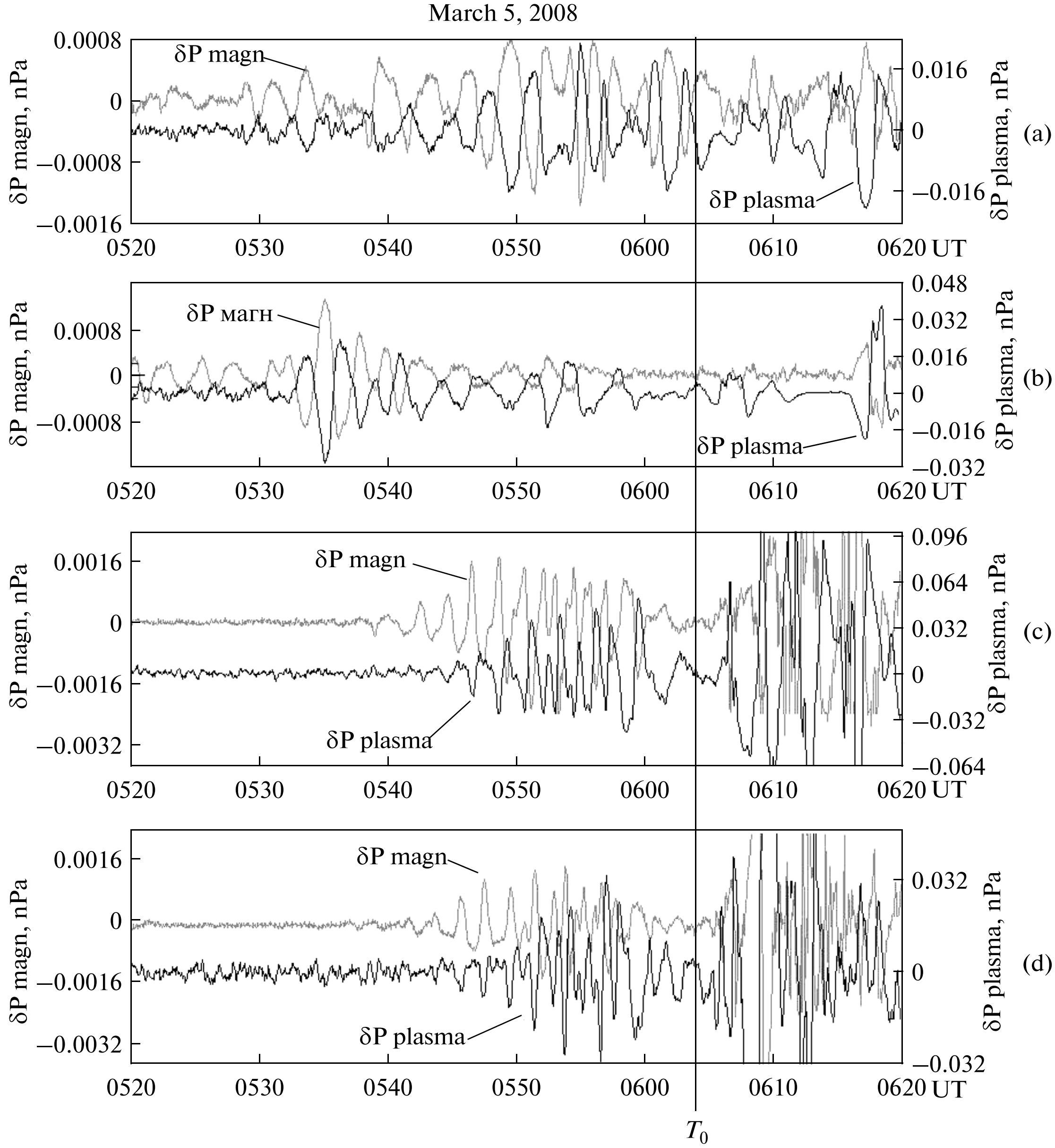

Fig. 2. Variations of magnetic (grey curve) and plasma (black curve) pressure observed by four THEMIS probes during 0520–0620 UT. Breakup onset identified by optical observations at GILL station is marked by the vertical line. The data are bandpass-filtered in the range 12–120 s.

between $P3$ and $P4$) under the assumption of earthward propagation.

We note that the above values of x are consistent with the propagation velocity of ballooning waves $k_{\parallel}^2$ derived from their dispersion relation [Golovchanskaya and Maltsev, 2005]

$$\omega^2 = V_{\mathrm{A}}^2 k_{\parallel}^2 + \omega_g^2 \frac{k_y^2}{k_x^2 + k_y^2}, \quad (1)$$

where ω is the frequency of perturbations, V_{A} the Alfvén velocity, $k_{\parallel}$ the parallel wave number, $\omega_g = \sqrt{2}\frac{v_{\mathrm{T}}}{a}$, v_{T} the proton thermal velocity (by THEMIS observations, $v_{\mathrm{T}} \sim 900$ km/s), a the half-thickness of the current sheet ($a \le 0.5R_{\mathrm{E}}$ for disturbed conditions), k_x and k_y the perpendicular wave numbers, the coordinates x and y refer to the equatorial plane. We note that small perpendicular scale sizes (large k_x) of our E-W perturbations justify the WKB approximation applied in the derivation of the dispersion relation (1). According to (1), propagation (from a source) of ballooning perturbations in the equatorial plane occurs in both radial and azimuthal directions. Taking from

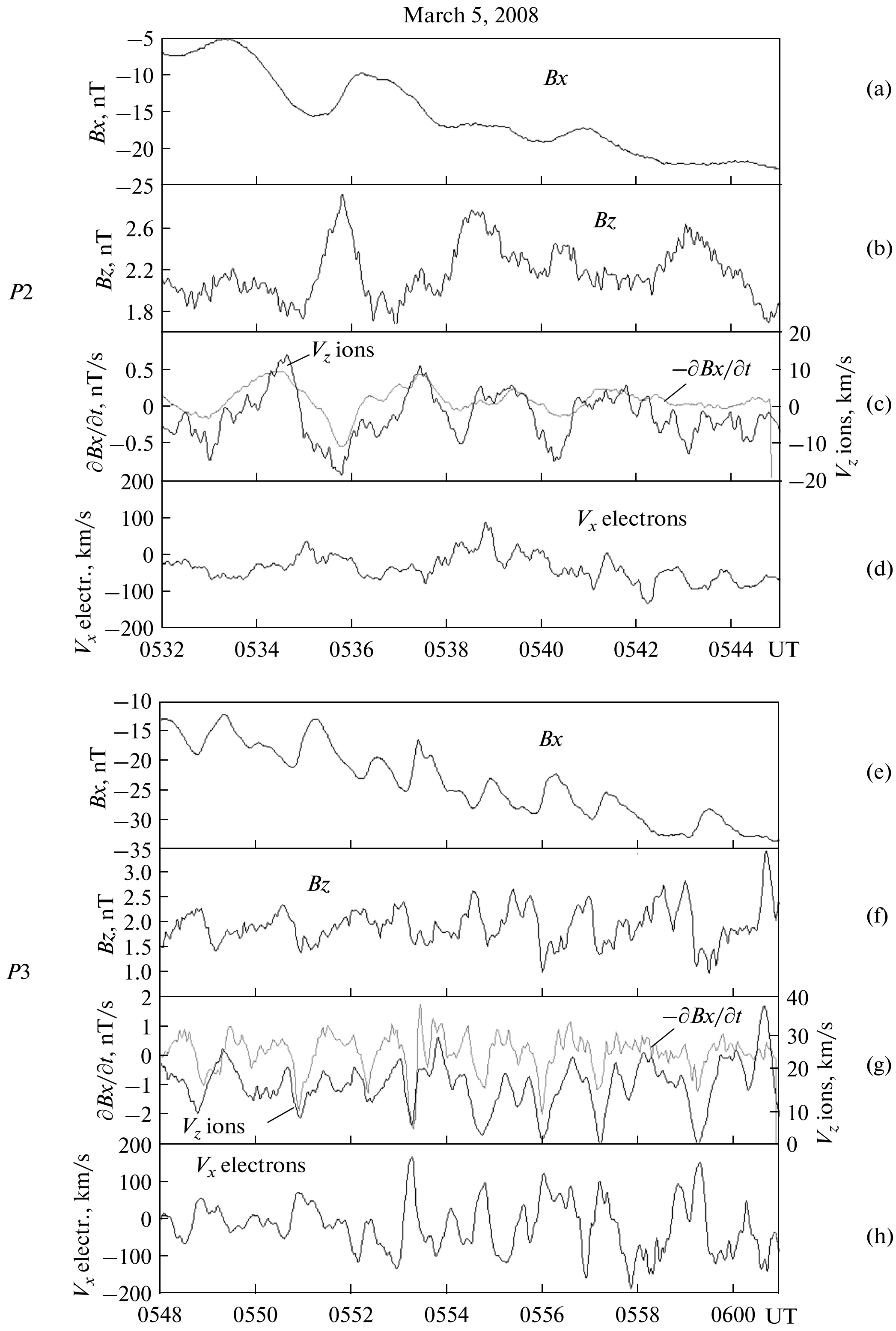

Fig. 3. Fluctuations in the *Bx* (a) and *Bz* (b) magnetic field components, (c) *z*-component of the ion velocity (black curve) along with $-\partial Bx/\partial t$ (grey curve), (d) V_x component of the electron velocity observed by *P*2. Similar data for *P*3 are shown in panels (e), (f), (g), (h).

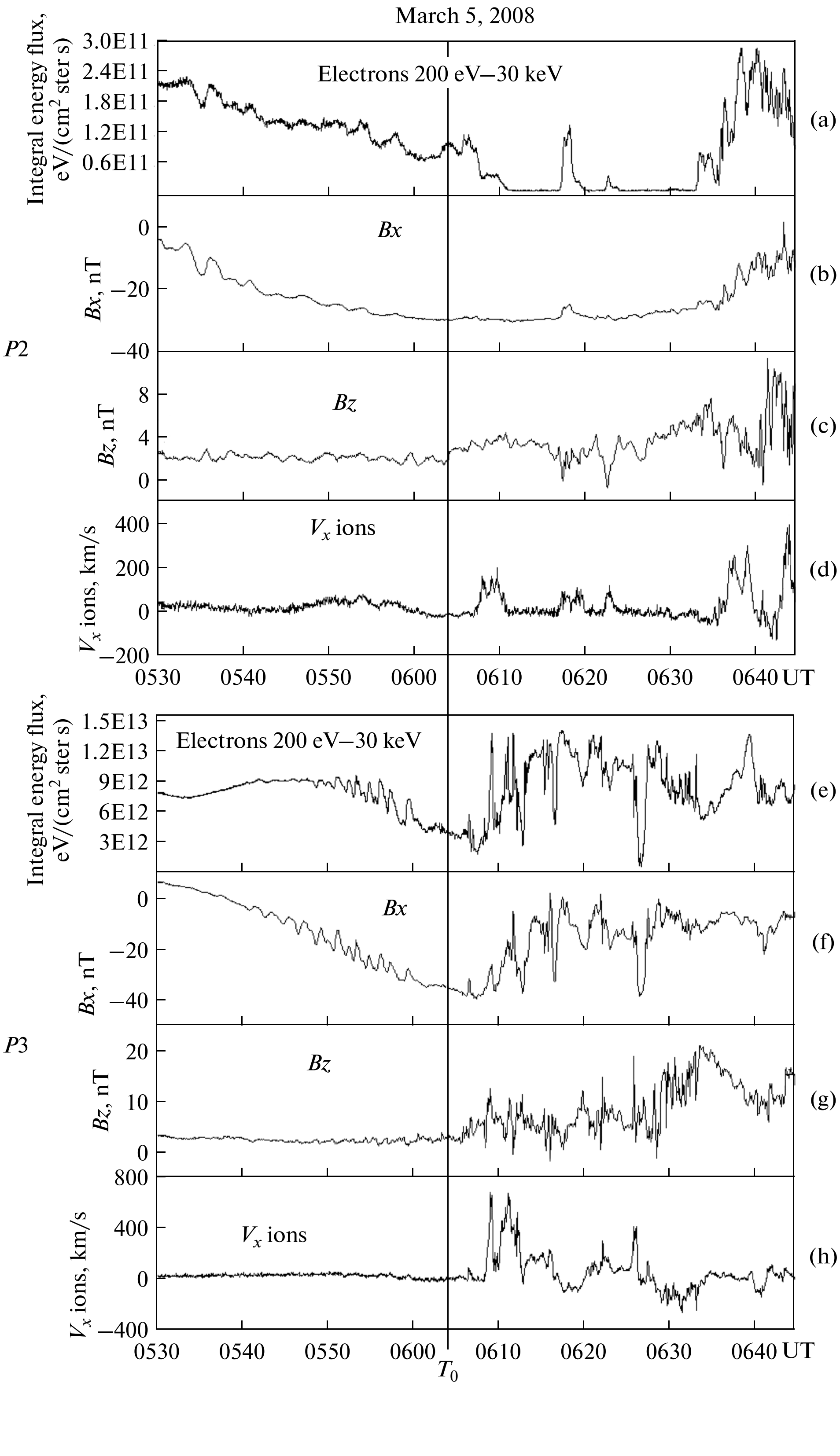

Fig. 4. Variations of integral energy flux of electrons in the energy range 200 eV–30 keV (a), *Bx* (b), and *Bz* (c) magnetic field components and *X*-component of the ion velocity (d) detected by *P*2. Similar data for *P*3 are shown in panels (e), (f), (g), (h).

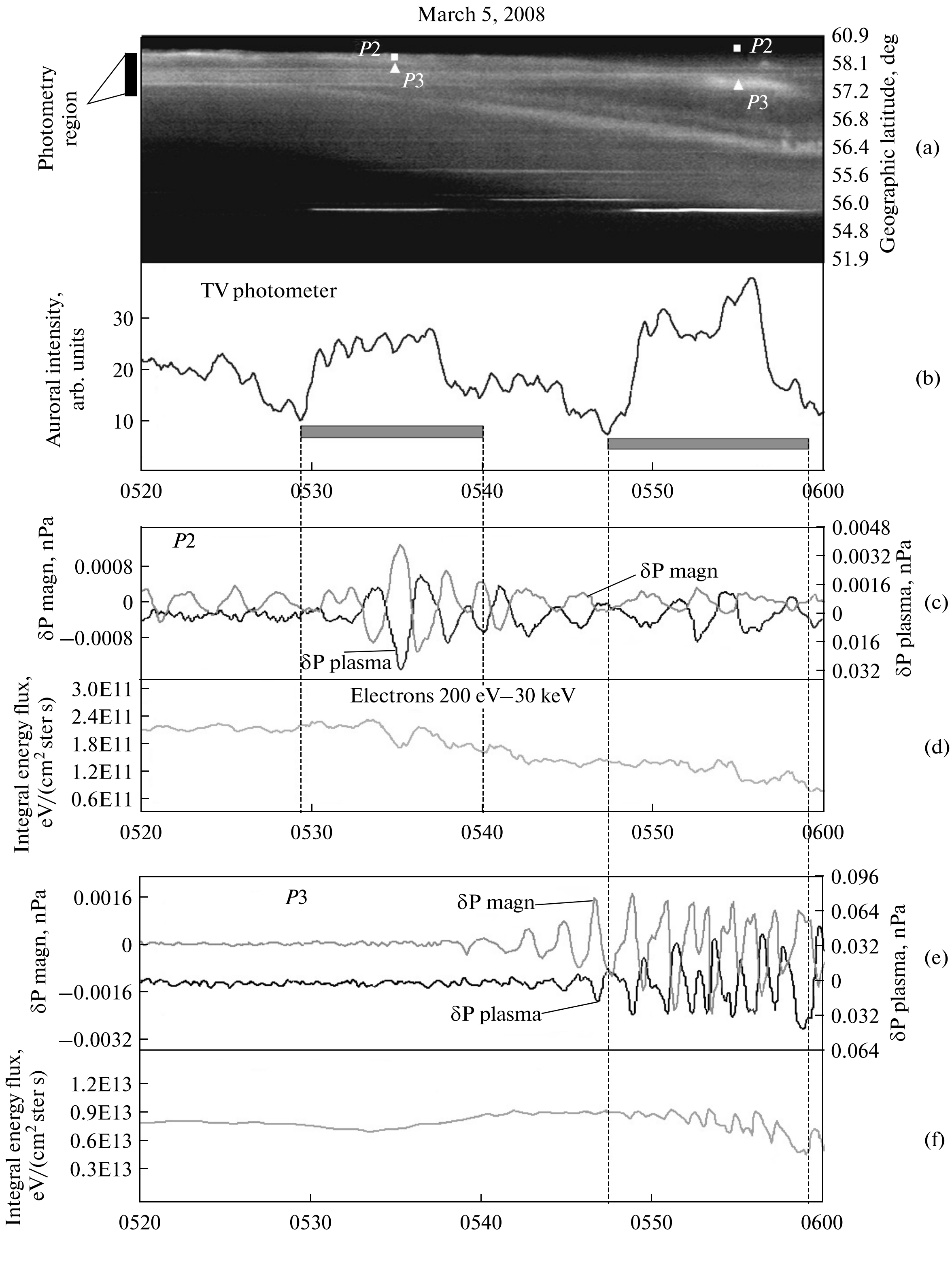

Fig. 5. A fragment of N-S keogram for GILL station in the time interval 0520–0600 UT (a), auroral intensity integrated over the photometry region (b), magnetic and plasma pressure measured by *P*2 (c) and *P*3 (e), integral energy flux of 200 eV–30 keV electrons, according to *P*2 (d) and *P*3 (f) observations.

optical observations the wavelength $\lambda_x = 2\pi/k_x \sim 20$–25 km in the ionosphere (0.25–0.3 R_E in the magnetosphere, according to T96 mapping), the ratio k_y/k_x, characterizing the wavefront inclination to the geomagnetic E-W direction, ~ 0.1–0.2 in the ionosphere (0.2–0.4 in the magnetosphere because of the difference in the radial and azimuthal magnetic convergence factors), $V_A \sim 10^2$ km/s, $k_{||} = (1–2)/a$, the earthward component of the ballooning wave propagation velocity derived from (1) is 30–40 km/s, consistent with observations.

To complete this section, we note that, as the considered perturbations are multiple, have large azimuthal extent, and propagate over large distance along the tail, possible inaccuracies in mapping do not seem very critical in our problem. Still, we have verified the conjugacy of optical and in-situ observations (Fig. 5). In Fig. 5a, a fragment of the keogram is shown for the time interval 0520–0600 UT (i.e., before T_0). The geographic latitudes of *P*2 and *P*3 footprints for 0535 UT and 0555 UT are marked on the meridian passing through the GILL zenith. Figure 5b shows the variations in the auroral intensity integrated by a virtual TV photometer over the region marked on the left in Fig. 5a. Grey rectangulars and vertical dotted lines indicate the time intervals when there were enhancements in the auroral intensity. At 0535 UT, *P*2 was in conjunction with the northern aurora, whereas *P*3—with the region free of auroras. During 0529:20–0540:00 UT, large-amplitude perturbations are observed by *P*2 (Figs. 5c, 5d), while *P*3 does not detect noticeable wave activity. At 0555 UT, *P*2 is not in conjunction with auroras. In this period *P*2 registers only weak magnetic and plasma variations, and decreasing integral energy flux of electrons. In contrast, *P*3 at 0555 UT is in conjunction with bright aurora and observes large-amplitude fluctuations at that time (Fig. 5e, Fig. 5f).

4. SUMMARY AND CONCLUSION

In this study, by ground-based optical observations, we investigated the dynamics of auroral breakup precursors in the period ~ 30–40 min before onset in an E-W event, according to the Mende et al. (2011) classification, and showed that it indicates a wave-like process (ftp://pgia.ru/kornilov/220301l4.avi; ftp://pgia.ru/kornilov/gill.avi). By conjunctive in-situ observations of four THEMIS probes in the plasma sheet, the underlying wave mode was identified as the ballooning mode. Having derived the characteristic scale-sizes and wavefront orientations of the ballooning perturbations in the magnetosphere from ionospheric auroral observations (with allowing for the magnetic convergence factor), we estimated the earthward component of propagation velocity from the ballooning wave dispersion relation as ~30–40 km/s.

It is commonly agreed that the appearance of a ballooning perturbation (i.e., a bubble or a bubble-blob pair) in the near-Earth tail provokes its destabilization and under certain conditions may trigger substorm. Previously it was suggested that ballooning-type perturbations can appear in the near tail either due to earthward floating plasma bubbles, as initially proposed by *Erickson and Wolf* [1980] and observationally evidenced by Baumjohann et al. (1989), Angelopoulos et al. (1992) and others, or in result of ballooning/interchange instability growth (e.g., Roux et al., 1991; Saito et al., 2008; Pritchett and Coroniti, 2010, 2011; Panov et al., 2012; Kozelova and Kozelov, 2013). The present study points to one more possibility, namely, that ballooning perturbations can be transported to the near tail by propagating ballooning waves.

ACKNOWLEDGMENTS

We acknowledge PGI staff for running aurora TV observations at Lovozero, Loparskaya and Tumanny, which were used for avi-films, V. Angelopoulos, C.W. Carlson, J.P. McFadden and S. Mende for the usage of aurora ground-base data from THEMIS Mission, and NASA NAS5-02099 contract for THEMIS probe data on fields and plasma. This work was supported by Program 9 of the Russian Academy of Sciences. We are grateful to Reviewer of this paper for helpful comments.

REFERENCES

Akasofu, S.-I., The development of auroral substorm, *Planet. Space Sci.,* 1964, vol. 12, pp. 273–282.

Akasofu, S.-I., Lui, A.T.Y., and Meng, C.-I., Importance of auroral features in the search of substorm onset processes, *J. Geophys. Res.*, 2010, vol. 115, p. A08218. doi:10.1029/2009JA014960

Angelopoulos, V., Baumjohann, W., Kennel, C.F., Coroniti, F.V., Kivelson, M.G., Pellat, R., Walker, R.J., Luehr, H., and Paschmann, G., Bursty bulk flows in the inner plasma sheet, *J. Geophys. Res.*, 1992, vol. 97, pp. 4027–4039.

Baumjohann, W., Paschmann, G., and Cattell, C.A., Average plasma properties in the central plasma sheet, *J. Geophys. Res.*, 1989, vol. 94, pp. 6597–6606. doi: 10.1029/JA094iA06p06597

Erickson, G.M. and Wolf, R.A., Is the steady convection possible in the Earth's magnetotail? *Geophys. Res. Lett.,* 1980, vol. 7, pp. 897–900.

Golovchanskaya, I.V. and Maltsev, Y.P., On the identification of the plasma sheet flapping waves observed by Cluster, *Geophys. Res. Lett.*, 2005, p. 32.L02102. doi: 10.1029/2004GL021552

Henderson, M.G., Kepko, L., Spence, H.E, Connors, M., Sigwarth, J.B., Frank, L.A., Singer, H.J., and Yumoto, K., The evolution of north-south aligned auroral forms into auroral torch structures: The generation of omega bounds and Ps6 pulsation via flow bursts, *Proc. the Sixth International Conference on Substorm*, Winglee, R.M., Ed., Seattle: Univ. of Washington, 2002, pp. 169–174.

Kornilova, T.A., Kornilov, I.A., and Kornilov, O.I., Auroral intensification structure and dynamics in the double oval: substorm of December 26, 2000, *Geomagnetizm i Aeronomiya*, 2006, vol. 46, no. 4, pp. 477–484.

Kornilova, T.A., Kornilov, I.A., and Kornilov, O.I., Fine structure of breakup development inferred from satellite and ground-based observations, *Ann. Geophys.*, 2008, vol. 26, pp. 1141–1148. doi:10.5194/angeo-26-1141-2008

Kornilova, T.A. and Kornilov, I.A., Counterstreaming auroral structures during substorm expansion, *J. Geophys. Res.*, 2012, vol. 117, p. A05328. doi:10.1029/2011JA017309

Kozelova, T.V. and Kozelov, B.V., Substorm-associated explosive magnetic field stretching near the earthward edge of the plasma sheet, *J. Geophys. Res.,* 2013, vol. 118, pp. 3323–3335. doi: 10.1002/jgra.50344

Liu, W., Physics of the explosive growth phase: Ballooning instability revisited, *J. Geophys. Res.*, 1997, vol. 102, pp. 4927–4931.

Mazur, N.G., Fedorov, E.N, and Pilipenko, V.A. Ballooning modes and their stability in a near-Earth plasma, *Earth Planet. Space*, 2013, vol. 65, pp. 463–471.

Mende, S.B., Frey, H.U., Angelopoulos, V., and Nishimura, Y., Substorm triggering by poleward boundary intensification and related equatorward propagation, *J. Geophys. Res.*, 2011, vol. 116, p. A00I31. doi:10.1029/2010JA015733

Miura, A., Ohtani, S., and Tamao, T., Ballooning instability and structure of diamagnetic hydromagnetic waves in a model magnetosphere, *J. Geophys. Res.,* 1989, vol. 94, pp. 15 231–15 242.

Nishimura, Y., Lyons, L., Zou, S., Angelopoulos, V., and Mende, S., Substorm triggering by new plasma intrusion: THEMIS all-sky imager observations, *J. Geophys. Res.*, 2010, vol. 115, p. A07222. doi:10.1029/2009JA015166

Oguti, T., Hydrogen emission and electron aurora at the onset of the auroral breakup, *J. Geophys. Res.*, 1973, vol. 78, pp. 7543–7547, p. doi:10.1029/JA078i031p07543

Ohtani, S. and Tamao, T., Does the ballooning instability trigger substorms in the near-Earth magnetotail?, *J. Geophys. Res.*, 1993, vol. 98, pp. 19 369–19 379.

Panov, E.V., Nakamura, R., Baumjohann, W., Kubyshkina, M.V., Artemyev, A.V., Sergeev, V.A., Petrukovich, A.A., Angelopoulos, V., Glassmeier, K.-H., McFadden, J.P., and Larson, D., Kinetic ballooning instability in a bent plasma sheet, *J. Geophys. Res.*, 2012, vol. 117, p. A06228. doi:10.1029/2011JA017496

Pritchett, P.L. and Coroniti, F.V. A kinetic ballooning/interchange instability in the magnetotail, *J. Geophys. Res.*, 2010, vol. 115, p. A06301. doi:10.1029/ 2009JA014752

Pritchett, P.L. and Coroniti, F.V., Plasma sheet disruption by interchange-generated flow intrusions, *Geophys. Res. Lett.*, 2011, vol. 38, p. L10102. doi:10.1029/2011GL047527

Rostoker, G., Lui, A.T.Y, Anger, C.D., and Murphree, J.S., North-south structures in the midnight sector auroras as viewed by the Viking imager, *Geophys. Res. Lett.*, 1987, vol. 14, pp. 407–410. doi:10.1029/GL014i004p00407

Roux, A., Perraut, S., Robert, P., Morane, A., Pedersen, A., Korth, A., Kremser, G., Aparicio, B., Rodgers, D., and Pellinen, R., Plasma sheet instability related to the westward traveling surge, *J. Geophys. Res.*, 1991, vol. 96, pp. 17697–17714.

Saito, M.H., Miyashita, Y., Fujimoto, M., Shinohara, I., Saito, Y., Liou, K., and Mukai, T., Ballooning mode waves prior to substorm-associated dipolarizations: Geotail observations, *J. Geophys. Res.*, 2008 vol. 35, p. 7103. doi:10.1029/2008GL033269

Uritsky, V.M., Liang, J., Donovan, E., Spanswick, E., Knudsen, D., Liu, W., Bonnell, J., and Glassmeier, K.H., Longitudinally propagating arc wave in the pre-onset optical aurora, *Geophys. Res. Lett.*, 2009, 36, L21103, doi:10.1029/2009GL040777